Theory of the Relaxation of Trapped Spin-States in Spin Crossover Materials: Drosophila for Complex Dynamics

M. Nadeem and Ben J. Powell*

School of Mathematics and Physics, The University of Queensland, Brisbane, Queensland, 4072, Australia

E-mail: powell@physics.uq.edu.au

Abstract

Understanding the underlying factors that give rise to complex kinetic processes is of fundamental interest to many research areas, such as protein folding, photochemistry, and quantum materials. Spin crossover (SCO) materials are relatively simple, highly tunable systems that offer a unique playground to study the universal aspects of complex dynamics. Experimentally, a diverse range of relaxation dynamics of trapped spin-states are observed in SCO materials, including exponential, sigmoidal, stretched exponential, multi-step, and mixed kinetics. Here we reproduce and explain this full range of relaxation behaviours using a semi-classical model that combines crystal field theory with elastic inter-molecular interactions. We show that frustrated intermolecular interactions lead to multiple energetically competitive ordered phases even in systems that contain only one crystallographically distinct SCO site. This rugged free energy landscape leads to dynamic disorder and thence complex dynamics. We show that the same frustrated interactions are responsible for multistep thermal transitions.

Introduction

Complex dynamic processes involving metastable states are of widespread interest across the chemical, physical and biological sciences. Such processes are key for understanding protein folding,[1] photochemical reactions,[2] and quantum materials.[3] Understanding the mechanisms of complex kinetics is a fundamental and essential step towards harnessing material functionalities for future applications, such as controlling chemical reactions,[4] rational drug design[5] and engineering multi-stable switches.[6,7] Key research goals[8] are: an overall understanding of complex mechanisms, the microscopic factors that control these processes, the properties of the intermediate metastable states, predicting decay timescales, and identifying rate-limiting steps. A traditional approach is to apply phenomenological master equations.[9] This divides complex kinetic processes into smaller steps, and a decay function with an associated rate constant characterizes each step. Reactions are classified into one-step or multiple steps processes. The master equation approach breaks down when the intermediaries are short-lived and cannot be divided into simple elementary steps.[10] An alternate approach is to consider complex processes globally and without the presumption of discrete steps.[11] This approach allows a systematic investigation of the driving factors and intermediaries of the processes. The later approach requires combining kinetic experiments and physics-based modelling.

The kinetics of biomolecules is particularly complex, protein folding is a prominent example. The frustrated interactions in native protein structures, strongly affect their free energy landscapes and give rise to intermediate metastable states.[12,13] A modern view on the theory of protein folding and protein function has two major ingredients, frustration and dynamic disorder.[12,13] Moreover, empirically, dynamic disorder correlates with higher levels of frustration.[12] However, biomolecules are large and complicated systems which greatly complicate modelling their behaviours. A practical approach to circumvent this would be to identify relatively simple systems in which these concepts can be studied. This approach has precedents from the idea of universality in physics to the use of model organisms in biology. Spin crossover (SCO) materials are ideal model systems for complex dynamics, as

elastic frustration causes a rugged free energy landscape, yet they are relatively simple and highly chemically tunable. A major theoretical challenge for modelling SCO materials is that multiple length scales need to be considered, as both intramolecular and intermolecular processes play vital roles in the dynamics.[14]

Coordination complexes of transition metals can have either low spin (LS) or high spin (HS) ground states.[15] Temperature-induced SCO ranges from a smooth crossover in solution to hysteric single-step and multi-step transitions in some solid-state materials.[16,17] One can also switch between spin-states by light, pressure, magnetic field, x-rays, and even nuclear decay.[18]

SCO materials exhibit a wide range of dynamic behaviours as they relax after light-induced spin-state trapping (LIESST).[18–29] This relaxation has been studied with two complementary experimental approaches. (1) In the isothermal kinetics approach, a sample is trapped in the HS state at a fixed temperature and evolution of the properties of the sample are monitored over time. (2) In thermally accelerated relaxation studies, the low-temperature trapped sample is slowly warmed while its properties are recorded.

Relaxation from metastable spin-states in SCO materials shows a wide range of dynamics. In solution, isothermal relaxation of an excited state is typically simple exponential.[19] This implies that the interactions between molecules do not influence decay rates or form. A sigmoidal form of decay is common in the solid state SCO.[20] This shows that cooperativity – due to elastic interactions between molecules – accelerates the kinetics. In the mean-field approximation, cooperative kinetics are described[20] by

$$\frac{d\gamma_{HS}}{dt} = -k_\tau \gamma_{HS} e^{\alpha(1-\gamma_{HS})}, \tag{1}$$

where k_τ is the rate constant, and α parametrizes the self-acceleration. Thus exponential and sigmoidal kinetics of spin-crossover materials are well understood within the single molecule[19] and mean-field pictures, respectively.[20]

Moreover, a wide variety of highly complex kinetics is also observed in SCO materials.[19–30] Slow relaxation, e.g., stretched exponential, is found in some materials,[21–23] while others exhibit a change of relaxation regime with temperature[24] or kinetics that are not consistent with simple rate models.[25–27] In some experiments, phenomenological descriptions of spin-crossover relaxation could only be obtained by mixing multiple decay functions to fit the observed decay.[24,28,29] These complex kinetics are observed in materials exhibiting both single-step[23] and multi-step[21,30] thermodynamic transitions.

It is important to note that complex kinetics are observed equally in SCO materials composed of a single species or multiple species.[29] In materials contain multiple distinct SCO sites, different intramolecular potential barriers for the trapped state to the ground state may give rise to multiple decay rates and non-linear kinetics. On the other hand, materials containing only one SCO species have uniform intramolecular physics and the observation of complex kinetics in these materials indicates a subtle role of collective effects beyond the mean-field that have not previously received a proper explanation.

Frustrated elastic interactions can drive spontaneous symmetry-breaking, intermediate spin-states having lower symmetry, in thermal SCO.[17,31,32] Kinetic experiments suggest that spontaneous symmetry-breaking also manifests in the relaxations of trapped spin-states in SCO materials.[10] Two-step relaxations from photo-induced HS states have been observed in several spin-crossover materials,[28,33,34] accompanied by lower symmetry intermediate states. Often a fast first step and a slower second step are observed, with each exhibiting different decay forms,[25,28,33,34] e.g., the isothermal relaxation of the trapped HS state in $[Fe(bppI)_2][BF_4]_2$ is two step: the first step decays exponentially but the second step decays sigmoidally.[25] In several experiments, intermediate plateaus have also been observed during thermally accelerated relaxation.[25,28,33–37] This indicates a relatively stable kinetically trapped intermediate phase.[35,36] Therefore, a systematic investigation of how elastic frustration leads to multistep kinetics and stabilises kinetically trapped symmetry-breaking intermediates is important for understanding the role of elastic frustration in SCO kinetics.

Theoretically, the mechanisms of complex relaxations are not described by single-molecule theory[19] or mean-field consideration of cooperativity.[20] The theory of thermal SCO has highlighted the significance of elastic cooperation and frustration,[17,32] particularly for the emergence of symmetry-breaking intermediate spin-states. Beyond mean-field theory, the dynamics of interacting spin-crossover molecules have been studied within Ising-like models using kinetic Monte Carlo,[38–41] with phenomenological parameters. This work highlighted the significance of short-range antiferroelastic interactions in driving two-step kinetics.[41] However, explaining the emergence of the vast range of dynamic behaviours of metastable states in the solid-state requires a theory beyond the phenomenological parameters and dynamics of Ising-like models. To comprehensively understand the fascinating body of SCO kinetic experiments requires a tractable model that captures both the single-molecular physics and collective effects.

Here we present molecular dynamics simulations of trapped phases using a recently developed semi-classical theory of spin-crossover material.[14] Our simulations naturally reproduce the observed complex relaxation behaviours and elucidate their controlling factors, particularly the role of frustration, i.e., interactions that cannot be simultaneously minimised. We show that the frustrated elastic interactions control the stability of intermediate trapped phases in SCO. This parallels the proposal that frustrated native interactions control intermediate states in protein folding.[12] We show that the emergence of dynamic disorder due to spin-state frustration drives complex kinetics of spin-crossover materials and discuss the generality of this mechanism in other systems.

Results and Discussion

Model

To study the collective dynamics of trapped spin-states, we recently developed a semi-classical approach to model spin-crossover materials.[14] In this method, the single-molecular

quantum chemistry, essential to describe the photoexcitation and relaxation behaviours, is combined with classical elastic interactions between molecules. We consider d^6 transition metal complexes with octahedral inner coordination spheres – archetypal spin-crossover compounds. For the effective theory, we include the three lowest energy states within the crystal field theory: $^1A_1$, $^3T_1$ and $^5T_2$, which we label LS, HS, and IS respectively. Many electron energies are parameterised with the Racah parameter, B, and ligand-field, Dq.[15] The spin-orbit coupling, ζ, allows the transition between the HS and LS states, mediated by the high energy IS state. Moreover, ζ introduces zero-field splittings between the 15-fold degenerate HS states.[14] We explicitly include the symmetric breathing coordinate of the metal-ligand octahedron, which is strongly coupled with the spin-states.[16] A harmonic potential, with a spring constant k, is assumed for the symmetric molecular vibration, and the minima of potential energies are set at $-\delta$ for LS, 0 for IS and δ for HS.

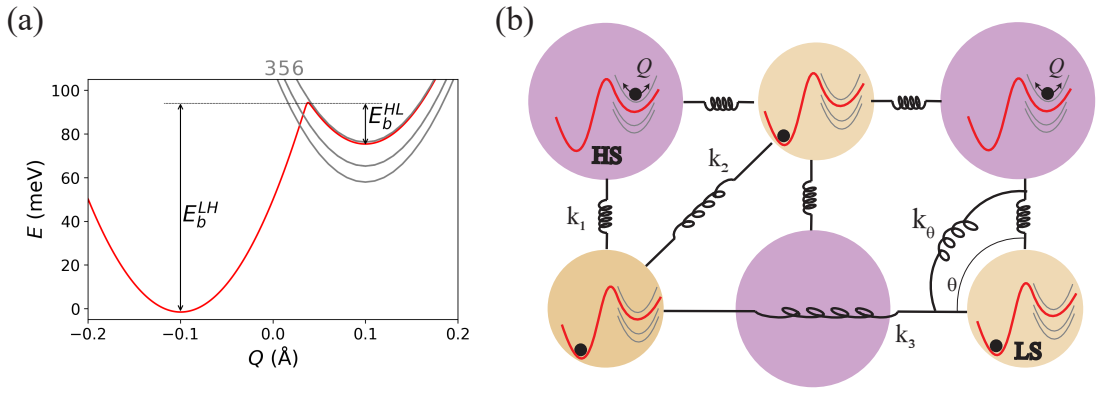

Fig. 1: **Schematic of the model.** (a) Potential energy surfaces, $V_\nu(Q)$, for a single molecule. For the double well (red), the barriers E_b^{HL} and E_b^{LH} that regulate the single molecular kinetics are labelled. The grey curves are pure HS levels, whose degeneracies are labelled. (b) Molecules form a square lattice with elastic intermolecular interactions defined in equation 2.

Typically, the LS and HS manifolds are much lower in energy than IS. Treating the spin-orbit coupling perturbatively, we integrate out high-energy IS state and diagonalise the resulting low-energy manifold of the system to obtain effective potential surfaces (PES); plotted, for typical parameter values (Extended Data Table 1), in Fig. 1a. Thus, the low-energy states[14] are a double well PES (red) with mixed LS, IS, and HS character, and 14

pure HS states (grey) split into three levels with degeneracies 3, 5 and 6.

We place N such spin-crossover centres on a square lattice with classical elastic interactions between neighbours, as sketched in Fig. 1. The model Hamiltonian is thus

$$H = \sum_{i}^{N} \left[\frac{\mathbf{p}_i^2}{2m} + \frac{\mathbf{P}_i^2}{2M} + V_\nu(Q_i) + \sum_{<i,j>_n} U_n(Q_i, Q_j, \mathbf{r}_i, \mathbf{r}_j) + \sum_{<i,j,k>_1} U_\theta(\mathbf{r}_i, \mathbf{r}_j, \mathbf{r}_k) \right], \quad (2)$$

where $V_\nu(Q_i)$ is an internal potential energy surface, $\mathbf{r}_i$ is position of the ith molecule, with mass m and conjugate momentum $\mathbf{p}_i$, and M is mass associated with the momentum P of the breathing coordinate Q. The elastic interaction between two nth nearest neighbours is given by

$$U_n = \frac{k_n}{2} \left(|\mathbf{r}_i - \mathbf{r}_j| - \mu_n(2\bar{d} + Q_i + Q_j) \right)^2, \quad (3)$$

where $\mu_1 = 1$, $\mu_2 = \sqrt{2}$, and $\mu_3 = 2$, and the harmonic potential associated with angular distortions is

$$U_\theta = \frac{k_\theta}{2} \sin^2 \left(\frac{\pi}{2} - \theta \right), \quad (4)$$

where θ is the angle between the nearest neighbour bonds, Fig. 1.

Typical parameters for SCO materials have previously been estimated.[14] Except as explicitly noted these parameters are used for all calculations in the paper. We solve the model on a 30×30 lattice using molecular dynamics (see methods). As the model has $30 \times 30 \times 3 = 2700$ degrees of freedom, explicit, direct mapping of free energy is not possible.

Mean-Field-like Kinetics

When all the interactions are ferroelastic ($k_n > 0$ for all n) there is no frustration. In this regime both the quasi-equilibrium behaviours and the relaxation dynamics are described by well-understood theories.[19,20] The relaxation of the trapped HS state is captured by mean-field theory (equation 1).

The LS and HS states have different magnetic susceptibilities, χ, at a temperature, T:

$\chi T \simeq 0$ in the LS state, whereas $\chi T \simeq 3\,\mathrm{cm^3\,K\,mol^{-1}}$ for the HS state.[16] Thus, a sigmoidal time dependence of χT signals mean-field-like relaxation from the HS phase to the LS phase (Fig. 2a). Weaker interactions, Fig. 2b, reduce cooperativity and hence the degree of self-acceleration, α. For vanishingly small intermolecular interactions $\alpha \to 1$ and the excited spin-state decay regains the simple exponential form characteristic of a single molecule.

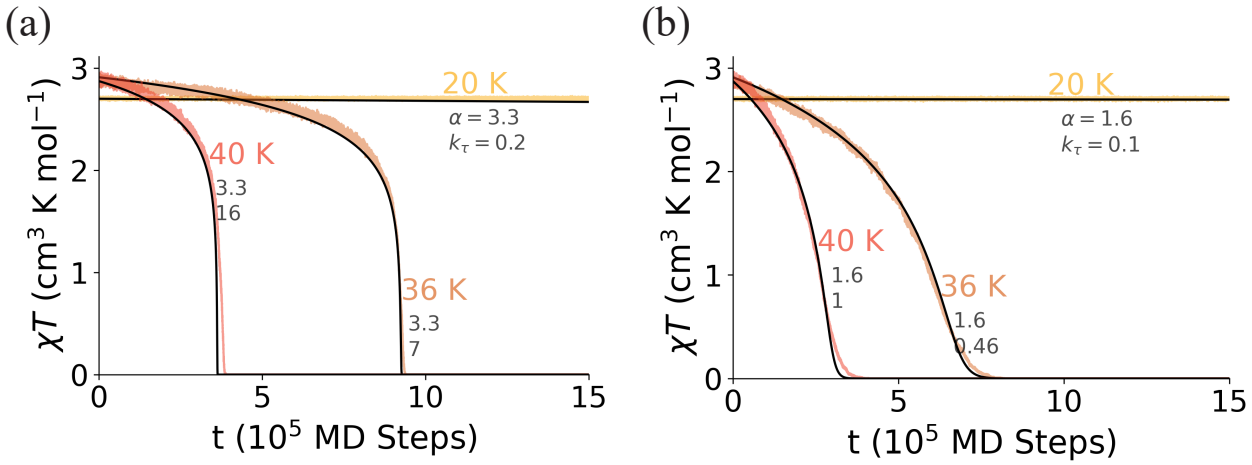

Fig. 2: **Mean-field-like isothermal relaxation from the trapped HS state in an unfrustrated system.** (a) The sigmoidal model (Eq. 1) fits the calculations well at all temperatures for unfrustrated interactions (e.g., the typical parameters listed in Extended Data Table 1, shown here). The parameters of the fits are given in the figure. (b) Lower interaction strengths, here $k_2 = 0.06k_1$ (versus $k_2 = 0.2k_1$ in (a)), decreases the cooperativity, which reduces k_τ and α.

In strongly cooperative unfrustrated systems we find a single step, first order transition in thermal sweeps, while thermally accelerated relaxation displays a single inflexion point in χT, Extended Data Fig. 1, which defines T_{LIESST}. As cooperativity is reduced, the hysteresis width decreases and, eventually, vanishes when the transition is replaced by a crossover. The thermally activated relaxation of trapped HS states shows a concomitant reduction in T_{LIESST} (Extended Data Fig. 1).

All of these behaviours are well understood on the basis of mean field theory. However, this description breaks down if the system is frustrated, below we show that this can lead to qualitatively different relaxation behaviours.

Weakly Frustrated Kinetics: Multi-Step Relaxation

In this section we demonstrate that weak elastic frustration can drive isothermal relaxations in two or more well-defined steps. Importantly, we demonstrate this in a model with a single SCO species – demonstrating that multiple SCO sites are not required for multistep relaxation. For example, weak frustration due to antiferroelastic third nearest neighbour interactions ($k_3 < 0$) leads to two-step relaxation of the trapped HS state, Fig. 3a. Both steps are sigmoidal. The intermediate plateau has short range stripe order with approximately half of the SCO centres in the HS state, Fig. 3b.

For this weakly frustrated system, thermal cycling shows a two-step transition with long-range stripe order in the intermediate plateau, Fig. 3c. The long-range order of the intermediate plateau spontaneously breaks the symmetry of crystal, doubling the unit cell length in one direction. However, as the kinetically trapped stripe state is short-lived thermally accelerated relaxation skips the intermediate plateau, yielding a single-step relaxation of the trapped HS state following LIESST, Fig. 3c.

A moderate increase in the frustration (making k_3 more negative) results in a longer lived intermediate state, Fig. 3d. At low temperatures, the HS $\rightarrow$ stripe decay remains sigmoidal (e.g., the 28 K data); but at higher temperatures, it becomes fast and takes a compressed-exponential form (e.g., the 52 K data). Nevertheless, the stripe $\rightarrow$ LS decay remains slow and sigmoidal in both temperature regimes. Similar two-step isothermal relaxations with a fast, exponential-like first step and a slower, sigmoidal second step have been observed in several materials,[25,28,33,34] $[Fe(isoq)_2\{Au(CN)_2\}_2]$, also shows a stripe intermediate plateau.[33]

Increased frustration leads to two-step thermally accelerated relaxation, Fig. 3f, with short-range stripe order in the intermediate plateau. Experimentally, two-step thermally accelerated relaxation has been observed in several spin-crossover materials.[28,33,34,36,37]

Two-step relaxation with chequerboard order in the intermediate plateau is found when k_2 is lowered, Extended Data Fig. 2. However, the change in the intermediate order does not lead to significant changes in the relaxation dynamics.

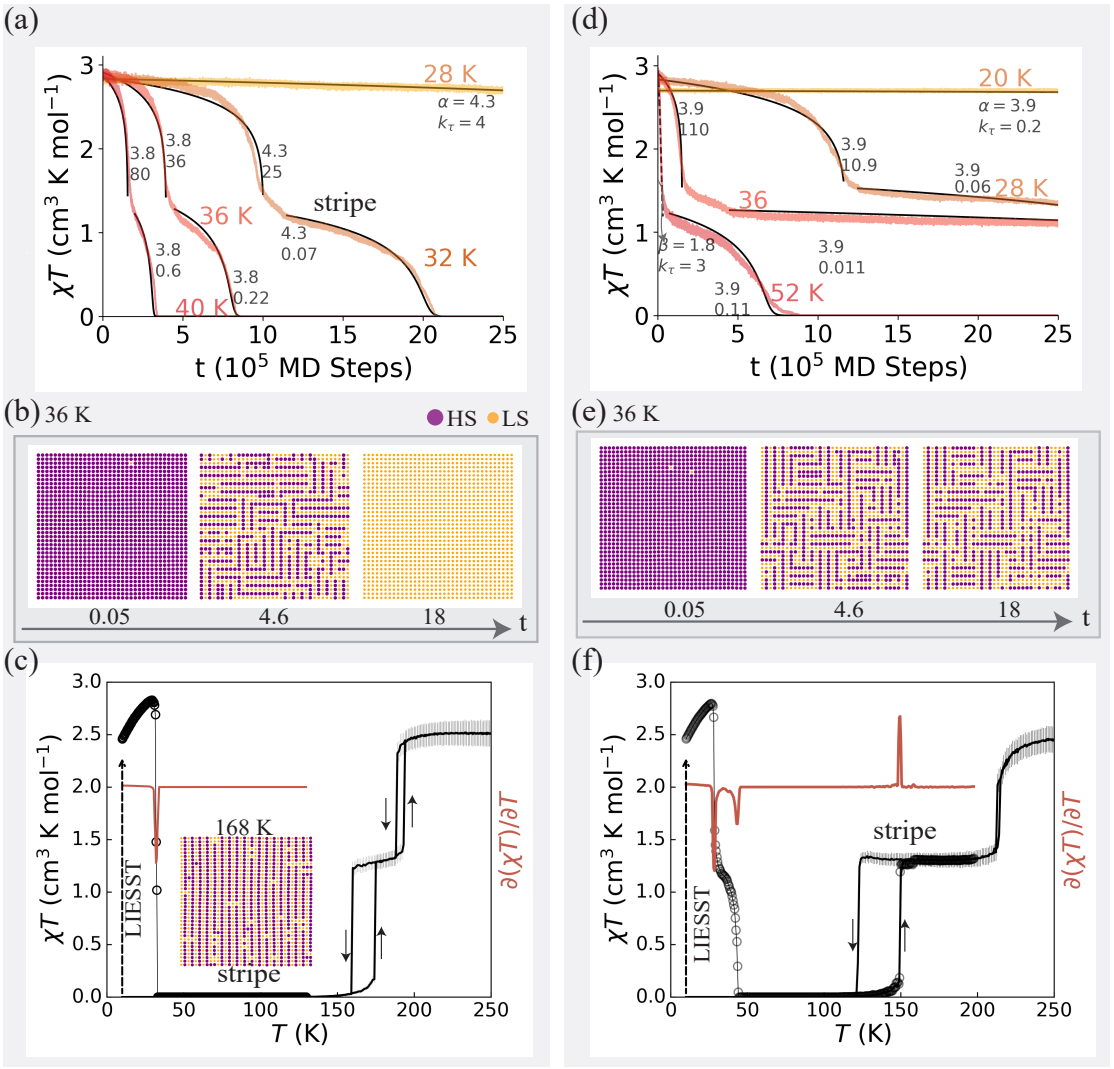

Fig. 3: Weak elastic frustration drives two step relaxation kinetics and two-step thermal transitions. (a,d) Two-step isothermal decay from the trapped HS state. (a) The metastable symmetry breaking phase in the intermediate plateau has short-range stripe order. At all temperatures, good sigmoidal fits can be found for both steps (solid lines). (d) Increased frustration stabilises the stripe phase. At 28 K, the decay is sigmoidal in both steps. At 52 K, the first relaxation step becomes compressed exponential, $e^{-k_\tau t^\beta}$ (dashed line), but the second step remains sigmoidal. This change occurs at ca. 46 K. (b,e) Corresponding evolution of spin-state configurations at 36 K. (c,f) Thermally accelerated relaxation of the trapped HS state (black circles) and SCO under thermal cycling (black lines). (c) Thermally accelerated relaxation following LIESST shows a single step characterized by a dip in $\partial(\chi T)/\partial T$ at $T_{\mathrm{LIESST}} = 32$ K (red line). Thermal SCO has an intermediate phase with long-range stripe order (inset). (f) The increased stability of the intermediate stripe phase (due to increased frustration) leads to two well-defined steps in the relaxation after LIESST, characterized by two dips in $\partial(\chi T)/\partial T$ at $T^{(1)}_{\mathrm{LIESST}} = 28$ K and $T^{(2)}_{\mathrm{LIESST}} = 44$ K, and increases the range of temperatures at which the intermediate phase is stable under thermal cycling. (a-c) $k_2 = 0.6k_1$ and $k_3 = -0.15k_1$. (d-f) $k_2 = 0.5k_1$ and $k_3 = -0.2k_1$.

The frustration is further enhanced if the nearest and next nearest neighbour interactions compete, for example, for antiferroelastic k_2. This can lead to three-step relaxation processes, as shown in Fig. 4, where the relaxation proceeds via two intermediate states. Again, longer-lived intermediate metastable states can also appearing during the thermally activated relaxation after LIESST. We are not aware of any experiment yet reporting three-step thermally assisted decay of a trapped HS state.

The corresponding thermal SCO is an incomplete two-step transition, with a low-temperature phase, $\gamma_{1/3}$, with HS fraction 1/3, and an intermediate spin-state phase, $\gamma_{2/3}$, with HS fraction 2/3. Both of these phases have lower symmetry than the high-temperature HS state. At low temperatures, reverse-LIESST, $\gamma_{1/3} \rightarrow$ LS, allows access to a hidden LS phase. Interesting the LS phase is also reached after thermally accelerated relaxation following LIESST. Similar behaviour has been observed in several SCO materials.[42,43]

To understand why the systems reaches the LS state after LIESST, but not on thermal cycling, it is important to recognise the differences in the spin-state configurations in the plateaus with a HS fraction $\gamma_{HS} = 1/3$. On thermal cycling the $\gamma_{1/3}$ phase has true long-range order (Fig. 4b). On thermal accelerated relaxation after LIESST we find a highly disordered state in the $\gamma_{HS} = 1/3$ plateau, with only short-range order. Importantly, this disorder varies in both space and time – that is, the disorder is dynamic. Our results indicate that the barrier between the long-range ordered $\gamma_{1/3}$ phase (Fig. 4b) and the LS phase is too large to be overcome in the relevant temperature range ($\lesssim 100$ K). However, the barrier between the disordered $\gamma_{HS} = 1/3$ state (Fig. 4d) and the LS phase is small enough to be overcome at $T^{(3)}_{\mathrm{LIESST}} = 82$ K. Thus, the dynamics of the disorder allows the system escape kinetic traps and access states that would otherwise be inaccessible. This may be an important general lesson for understand other dynamically disorder systems. For example, it is interesting to compare this with the functional advantage dynamic disorder is believed to provide proteins with in binding to specific substrates.[12]

On lowering the frustration (e.g., making k_2 less negative), the intermediate metastable

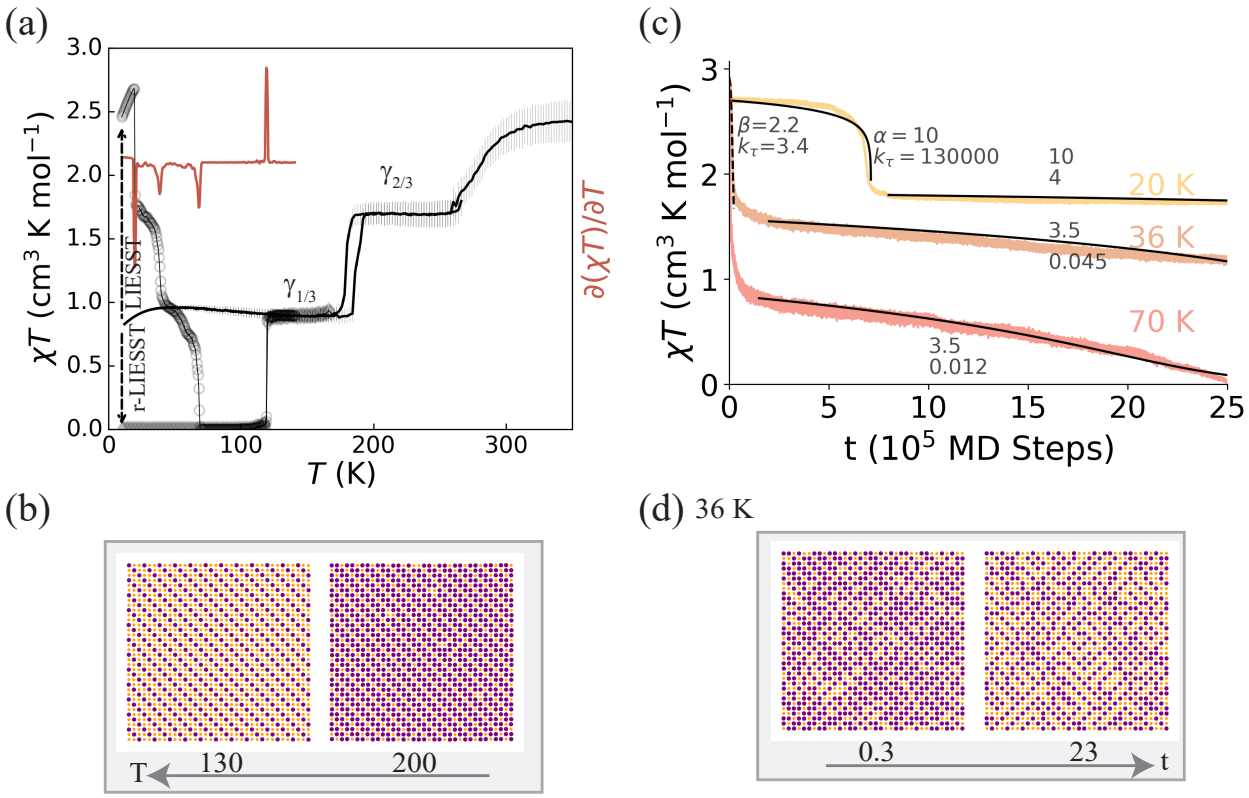

Fig. 4: **Three-step thermally accelerated relaxation and two-step incomplete thermal transitions in a highly frustrated system.** (a) Thermally accelerated relaxation of the low-temperature trapped HS state proceeds via two intermediate plateaus (black circles). This leads to three negative peaks in $\partial(\chi T)/\partial T$ (red line) at $T^{(1)}_{\text{LIESST}} = 22$ K, $T^{(2)}_{\text{LIESST}} = 40$ K and $T^{(3)}_{\text{LIESST}} = 82$ K. Thermal SCO (black lines) shows as incomplete two-step transition with long-range ordered phases in the intermediate plateau ($\gamma_{2/3}$) and low-temperature phase ($\gamma_{1/3}$). The LS phase is accessible via reverse-LIESST at 10 K, and relaxes to the $\gamma_{1/3}$ phase at $T_{\text{r-LIESST}} = 120$ K, yielding a peak in $\partial(\chi T)/\partial T$. (b) Typical spin-state configurations of the $\gamma_{1/3}$ (at 130 K) and $\gamma_{2/3}$ (at 200 K) phases on cooling from high temperature. (c) Calculated isothermal relaxations of the trapped HS state at various temperatures show that intermediate steps are stable for long times. This is clearly responsible for the multi-step thermally accelerated relaxation. (d) The spin-state configurations during relaxation at 36 K show significant disorder, unlike the orderly configurations observed during thermal crossover (b). This suggests that at low temperatures the LS phase is thermodynamically stable and the dynamic disorder following thermally accelerated relaxation prevents the system from becoming kinetically trapped in the $\gamma_{1/3}$ phase, as it does on thermal cycling. Here $Dq/B = 2.0459$, $k_1 = 1.55$ eV/Å^2, $k_2 = -0.33k_1$, $k_3 = 0.11k_1$, and $k_\theta = 0.56k_1$.

states become less stable, erasing the intermediate plateaus in the thermally activated relations after LIESST and allowing direct access to the LS phase on thermal cycling, Extended Data Fig. 3.

Complex Kinetics: Dynamic Disorder from Competing Orders

In highly frustrated systems we find significantly altered kinetic processes as well as multistep relaxation. We observe that multiple intermediate ordered states are competitive, indicating that free energy landscape is rugged. Furthermore, we observe that dynamic spin-state disorder, due to this ruggedness, causes complex relaxation kinetics, Figs. 5, 6.

Intermediate orders compete in broad parameter ranges of the semi-classical model and even when the thermally accelerated decay and thermal spin-crossover are both single-step, as shown in Fig. 5. We find that in these parameter ranges the calculated χT cannot be fit by standard phenomenological rate models, Fig. 5a. At intermediate temperatures (ca. 30-40 K), no single simple relaxation form fits the isothermal relaxation data well.

A common behaviour (seen, for example, in the 34 K data in Fig. 5) is that χT initially relaxes sigmoidally, but at longer times the relaxation slows and can be fit by a stretched exponential function, $e^{-k_\tau t^\beta}$ with $\beta < 1$. Experimentally, such 'mixed relaxations' have been observed in several SCO materials.[21,25,28,29,29] For example, $[Fe(bppSMe)_2][BF_4]_2$ exhibits behaviour similar to the calculations presented in Fig. 5: single step SCO, a single negative peak in $\partial(\chi T)/\partial T$, and mixed isothermal kinetics with stretched tails.[25] We observe complex relaxation dynamics with temperature dependent regime changes for many other parameter regimes with a wide range of intermediate incipient orders.

It has been speculated that such complex kinetics require materials with multiple crystallographically distinct SCO centres.[24,25,28] However, our result shows that mixed relaxation can occur with only one spin-crossover species, consistent with experiment.[29] Snapshots of spin-state distributions during the relaxation reveal small areas of four metastable spin-state orders: stripe, chequerboard, $\gamma_{1/4}$ and $\gamma_{3/4}$, Fig. 5b. None of these phases stabilizes into

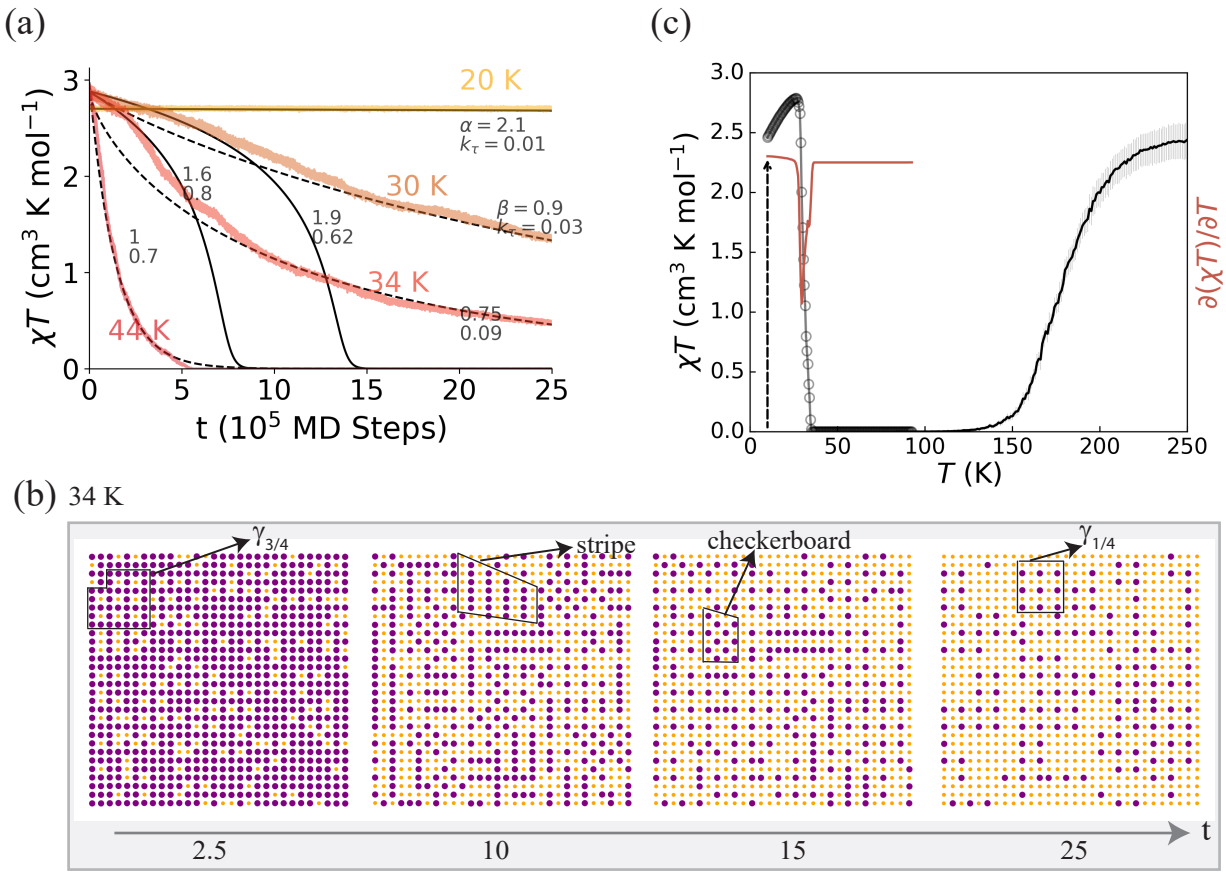

Fig. 5: **Complex isothermal relaxation from a rugged free energy landscape and dynamical disorder due to competing phases in a model with a single SCO species.** (a) Isothermal relaxation slows as it proceeds. At short times and low temperatures the relaxation is sigmoidal (equation 1; solid line); at low times and high temperatures the relaxation follows a stretched exponential form ($e^{k_\tau t^\beta}$, $\beta < 1$; dashed line). (b) The spin-state evolution at 34 K shows microdomains domains of competing checkerboard, stripe, $\gamma_{1/4}$ and $\gamma_{3/4}$ phases. (c) For these parameters, thermal SCO and thermally activated relaxation are both single-step processes. Here $k_3 = -0.15k_1$.

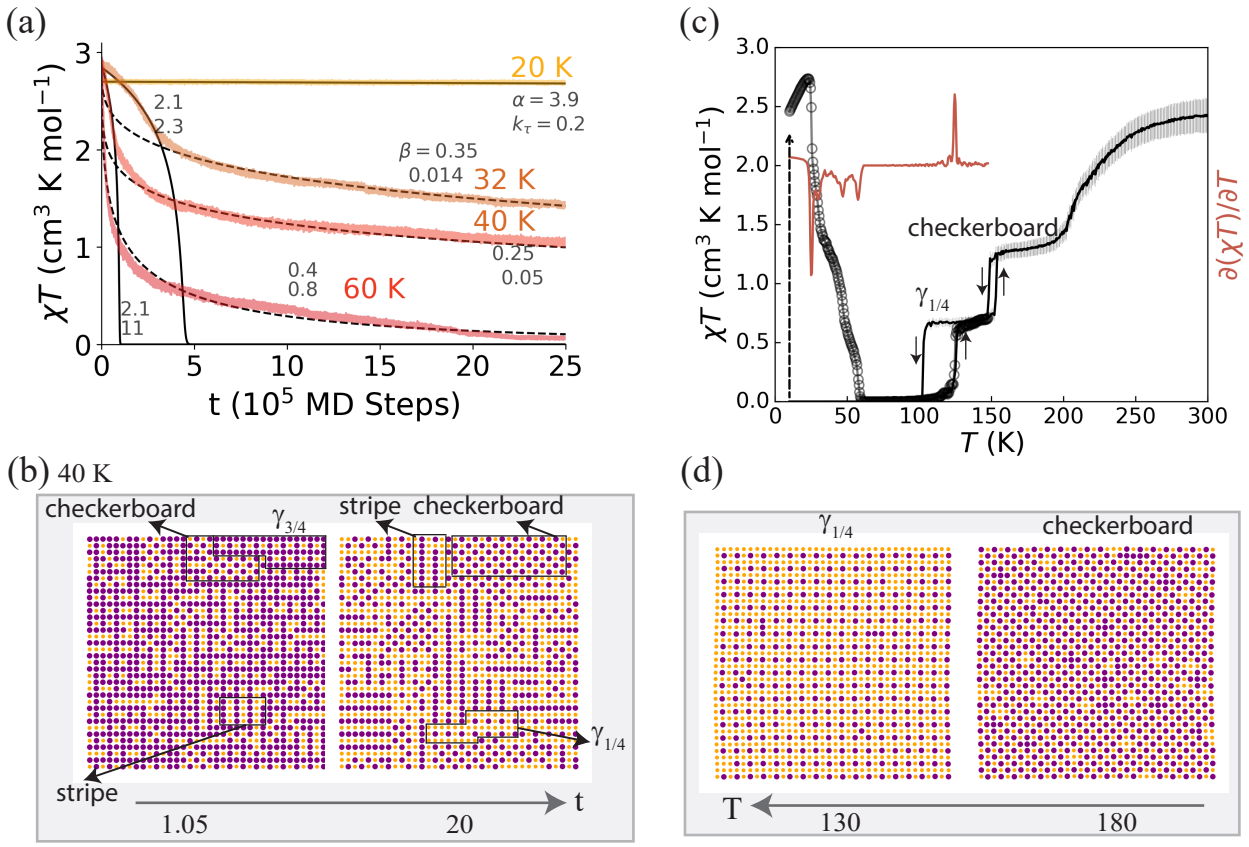

Fig. 6: **A rugged free energy landscape leading to complex isothermal relaxation, multistep thermally assisted relaxation, and multistep the thermal SCO.** (a) Isothermal relaxation is sigmoidal at short times and low temperatures (equation 1; solid line) but becomes stretched exponential ($e^{k_\tau t^\beta}$, $\beta < 1$; dashed line) at long times and high temperatures. (b) Snapshots of the spin-state distributions during the isothermal relaxation at 40 K show competing domains of stripe, checkerboard, $\gamma_{1/4}$ and $\gamma_{3/4}$ spin-state orders. (c) The thermally accelerated decay of the trapped HS state is extremely complicated, $\partial(\chi T)/\partial T$ shows several well defined negative peaks and multiple subtle dips. Thermal SCO proceeds via two long-range ordered intermediate phases, $\gamma_{1/4}$ and checkerboard. (d) Typical snapshots at the SCO steps on cooling from high temperatures. Here $k_2 = 0.23k_1$ and $k_3 = -0.2k_1$.

long-range order or lives for long times. However, the competition between these incipient orders leads to a dynamic spin-state disorder, resulting in a complex relaxation process, where the trapped spin-state initially decays rapidly, but later decay is frustrated by the need to disentangle the competing orders, dramatically slowing the decay to $\gamma_{\mathrm{HS}} = 0$.

For even more highly frustrated systems the free energy landscape is even more rugged. This leads to more complicated dynamics because the competing intermediate states are stable on longer timescales. An example with four incompatible incipient spin-state orders with multiple steps is shown in Fig. 6. In comparison to the single step case, Fig. 5a, the more stable dynamic disorder induces stretched exponetial relaxation at high temperatures, e.g, the 60 K data in Fig. 6a. Such high temperature stretched relaxation is often observed in SCO materials.[21,29]

Signatures of competing orders are also be found in thermal SCO and thermally accelerated relaxation, Fig. 6c. Competing orders lead to poorly defined steps in thermally accelerated decay, highly reminiscent of the behaviors of $[\mathrm{Fe}[(\mathrm{Hg(SCN)_3})_2](4{,}40{-}\mathrm{bipy})_2]_\mathrm{n}$ and $\mathrm{Fe(py)_2[Ag(CN)_2]_2}$.[29,36,44] Here the corresponding thermal SCO, Fig. 6b, has two well defined intermediate steps: at $\gamma_{\mathrm{HS}} = 1/2$ and $1/4$ with chequerboard and $\gamma_{1/4}$ states respectively. The chequerboard phase has significantly more disorder than we found in the weakly frustrated cases discussed above. This is highly reminiscent of $\mathrm{Fe(py)_2[Ag(CN)_2]_2}$, which exhibits an incomplete two-step thermal SCO with a disordered phase at the intermediate plateau and complex isothermal HS $\rightarrow$ LS relaxations with stretched form at later times during the decay.[29,44]

Conclusion

We have used a semi-classical theory to understand and characterise the dynamics of frustrated, dynamically disordered SCO materials beyond standard phenomenological approaches. It is important that this model describes intramolecular processes and intramolecular elastic

interactions on an equal footing. Both play key roles in the dynamics of SCO materials: the potential barriers in single molecules, Fig. 1, sets the basic timescales for dynamic processes, while intermolecular elastic interactions stabilise the intermediate phases, which can lead to dynamics that are slow on the basic molecular timescale.

This theory has enabled us to explain the emergence of a range of isothermal relaxation behaviours of the trapped states including sigmoidal, stretched, compressed exponential, and mixed relaxation. These occur because elastic interactions introduce (metastable) ordered phases that can act as kinetic traps, greatly complicating the relaxation dynamics.

We have also shown that dynamical disorder allows the system to escape kinetic traps. This explains why SCO materials that show incomplete transitions often relax to the LS phase after LIESST. The thermal intermediate plateau is long-range ordered and therefore significantly more stable than the dynamically disordered intermediate plateau reached on thermally accelerated relaxation following LIESST. This has clear parallels to the selective advantages provided to proteins by dynamic disorder.

In elastically frustrated SCO materials, multiple competing incipient orders give rise to rugged free energy landscapes. This ruggedness results in dynamically disordered spin-state configurations and hence explains the changes in relaxation regime with temperature seen experimentally in SCO materials.[24] For example, the, frequently observed, quantitative and qualitative slowing of the relaxation at long times can be understood as the system becomes stuck in these metastable states. The rugged free energy landscapes are also responsible for multistep isothermal decay, multistep thermally activated relaxation, and multistep thermal SCO. For the latter two of these it is crucial to recall that the relative stability of different many-body states changes with temperature.

Previously, complex relaxation kinetics have often been attributed to non-uniform SCO species or sample impurities.[24,25,28] However, we find the full range of kinetic behaviours observed experimentally in a model with only one species of SCO complexes.

Chemically, SCO materials are highly tunable. This positions SCO materials as outstand-

ing model systems to study complex dynamics. This is potential is significantly enhanced by the relatively simple theory, presented here, explaining the experiments. In the future, these materials may help to establish a universal understanding of these concepts in broader contexts, from biomolecular dynamics to quantum materials. In particular, the current approach of integrating out the local quantum effects, to give a classical Marcus-Hush like PES, while retaining interactions between subunits on longer length scales could be a useful first step for understanding the complex dynamics due to frustration and dynamic disorder in a wide range of materials.

Many porous SCO frameworks have been synthesised.[45] These frameworks allow the absorption of a range of guest molecules, which can significantly alter the physics of SCO.[45–47] Therefore, it is interesting to speculate whether dynamic disorder due to competing ordered states in such frameworks could enable behaviours analogous to fuzzy (adaptable) binding in proteins.

Method

We simulate the system with molecular dynamics (MD) at a constant temperature, a constant pressure and a constant number of molecules on a 30×30 square lattice, using the Nose-Hoover thermostat and the Anderson barostat.[48] Separate thermostats are applied for lattice and internal coordinates to circumvent the flying ice cube problem.[49] We assume barrierless transitions within HS states, and the thermal occupancy of the internal PESs is determined by applying 20 Metropolis Monte Carlo steps after every 50 MD steps.

To simulate isothermal kinetic experiments, we initialize the simulation in an all-HS state at the set temperature, then we let the ensemble evolve in time at constant temperature for 2.5×10^6 MD steps. The change in the magnetic response, χT, of a sample with time and temperature is calculated, where χ is magnetic susceptibility. In the thermally accelerated approach, light is used to prepared a sample in a trapped phase at 10 K, once the light

is switched off, the sample is heated until it decays to LS.[50] To simulate this, we initialize at HS and let the molecular dynamics evolve to 5.5×10^5 MS steps at a set temperature and increase the temperature by 0.5 K. Experimentally, HS→LS relaxation timescales vary widely: from extremely fast to many hours.[21–23,25–29] The microscopic variation of the model parameters allows us to set a small single molecular energy barrier to the trapped states (shown in Fig. 1a) without significantly changing the other physics of the problem. This allows us to probe the dynamics of these materials within computable timescales and without numerically accelerating the calculations.

For thermal SCO, the sample is initialized in the all-HS state at a high temperature, cooled down to 10 K, and then heated to the initial high temperature. For thermal SCO, the temperature is changed in 1.0 K intervals.

Acknowledgments

It is a pleasure to acknowledge helpful conversations with Cameron Kepert, Ross McKenzie, Suzanne Neville, and Shuang Yaun. This work was supported by the ARC through project DP200100305. M. Nadeem was supported by an Australian Government Research Training Program Scholarship.

References

(1) Dill, K. A.; MacCallum, J. L. The protein-folding problem, 50 years on. *Science* **2012**, *338*, 1042–1046.

(2) Pathak, S.; Ibele, L. M.; Boll, R.; Callegari, C.; Demidovich, A.; Erk, B.; Feifel, R.; Forbes, R.; Di Fraia, M.; Giannessi, L., et al. Tracking the ultraviolet-induced photochemistry of thiophenone during and after ultrafast ring opening. *Nat. Chem.* **2020**, *12*, 795–800.

(3) Zong, A.; Nebgen, B. R.; Lin, S.-C.; Spies, J. A.; Zuerch, M. Emerging ultrafast techniques for studying quantum materials. *Nat. Rev. Mater.* **2023**, *8*, 224–240.

(4) Sanchez, D. M.; Raucci, U.; Martínez, T. J. In silico discovery of multistep chemistry initiated by a conical intersection: the challenging case of donor-acceptor stenhouse adducts. *J. Am. Chem. Soc.* **2021**, *143*, 20015–20021.

(5) Parrill, A. L.; Reddy, M. R. *Rational drug design: novel methodology and practical applications*; ACS Publications, 1999; Chapter 1.

(6) Chi, Y.; Li, Y.; Zhao, Y.; Hong, Y.; Tang, Y.; Yin, J. Bistable and multistable actuators for soft robots: structures, materials, and functionalities. *Adv. Mater.* **2022**, *34*, 2110384.

(7) Delgado, T.; Tissot, A.; Guénée, L.; Hauser, A.; Valverde-Muñoz, F. J.; Seredyuk, M.; Real, J. A.; Pillet, S.; Bendeif, E.-E.; Besnard, C. Very long-lived photogenerated high-spin phase of a multistable spin-crossover molecular material. *J. Am. Chem. Soc.* **2018**, *140*, 12870–12876.

(8) Klippenstein, S. J.; Pande, V. S.; Truhlar, D. G. Chemical kinetics and mechanisms of complex systems: a perspective on recent theoretical advances. *J. Am. Chem. Soc.* **2014**, *136*, 528–546.

(9) Fernández-Ramos, A.; Miller, J. A.; Klippenstein, S. J.; Truhlar, D. G. Modeling the kinetics of bimolecular reactions. *Chem. Rev.* **2006**, *106*, 4518–4584.

(10) Chorazy, S.; Charytanowicz, T.; Pinkowicz, D.; Wang, J.; Nakabayashi, K.; Klimke, S.; Renz, F.; Ohkoshi, S.-i.; Sieklucka, B. Octacyanidorhenate(v) ion as an efficient linker for hysteretic two-step iron(ii) spin crossover switchable by temperature, light, and pressure. *Angew. Chem. Int. Ed.* **2020**, *59*, 15741–15749.

(11) Buchner, G. S.; Murphy, R. D.; Buchete, N.-V.; Kubelka, J. Dynamics of protein folding: Probing the kinetic network of folding–unfolding transitions with experiment and theory. *Biochim. Biophys. Acta, Proteins Proteomics* **2011**, *1814*, 1001–1020.

(12) Gianni, S.; Freiberger, M. I.; Jemth, P.; Ferreiro, D. U.; Wolynes, P. G.; Fuxreiter, M. Fuzziness and frustration in the energy landscape of protein folding, function, and assembly. *Acc. Chem. Res.* **2021**, *54*, 1251–1259.

(13) Fuxreiter, M. Fuzziness in protein interactions—a historical perspective. *J. Mol. Biol.* **2018**, *430*, 2278–2287.

(14) Nadeem, M.; Cruddas, J.; Ruzzi, G.; Powell, B. J. Toward high-temperature light-induced spin-state trapping in spin-crossover materials: the interplay of collective and molecular effects. *J. Am. Chem. Soc.* **2022**, *144*, 9138–9148.

(15) Sugano, S.; Tanabe, Y.; Kamimura, H. *Multiplets of transition-metal ions in crystals*; Academic Press, 1970.

(16) Gütlich, P.; Goodwin, H. A. In *Spin crossover in transition metal compounds I*; Gütlich, P., Goodwin, H., Eds.; Springer Berlin Heidelberg: Berlin, Heidelberg, 2004; pp 1–47.

(17) Cruddas, J.; Powell, B. J. Structure–property relationships and the mechanisms of multistep transitions in spin crossover materials and frameworks. *Inor. Chem. Front.* **2020**, *7*, 4424–4437.

(18) Chastanet, G.; Lorenc, M.; Bertoni, R.; Desplanches, C. Light-induced spin crossover—Solution and solid-state processes. *Comptes Rendus Chimie* **2018**, *21*, 1075–1094.

(19) Hauser, A. Intersystem crossing in Fe(II) coordination compounds. *Coor. Chem. Rev.* **1991**, *111*, 275–290.

(20) Hauser, A.; Jeftić, J.; Romstedt, H.; Hinek, R.; Spiering, H. Cooperative phenomena and light-induced bistability in iron(II) spin-crossover compounds. *Coor. Chem. Rev.* **1999**, *190-192*, 471–491.

(21) Buron-Le Cointe, M.; Ould Moussa, N.; Trzop, E.; Moréac, A.; Molnar, G.; Toupet, L.; Bousseksou, A.; Létard, J. F.; Matouzenko, G. S. Symmetry breaking and light-induced spin-state trapping in a mononuclear Fe^{II} complex with the two-step thermal conversion. *Phys. Rev. B* **2010**, *82*, 214106.

(22) Enachescu, C.; Linares, J.; Varret, F.; Boukheddaden, K.; Codjovi, E.; Salunke, S. G.; Mukherjee, R. Nonexponential relaxation of the metastable state of the spin-crossover system $[Fe(L)_2(ClO_4)_2.H_2O$ [L= 2,6-Bis(pyrazole-1-ylmethyl)pyridine]. *Inor. Chem.* **2004**, *43*, 4880–4888.

(23) Mishra, V.; Mukherjee, R.; Linares, J.; Balde, C.; Desplanches, C.; Létard, J.-F.; Collet, E.; Toupet, L.; Castro, M.; Varret, F. temperature-dependent interactions and disorder in the spin-transition compound $[FeII(L)_2][ClO_4]_2.C_7H_8$ through structural, calorimetric, magnetic, photomagnetic, and diffuse reflectance investigations. *Inor. Chem.* **2008**, *47*, 7577–7587.

(24) Chastanet, G.; Sciortino, N. F.; Neville, S. M.; Kepert, C. J. High spin to low spin relaxation regime change in a multistep 3d spin-crossover material. *Eur. J. Inorg. Chem.* **2018**, *2018*, 314–319.

(25) Kershaw Cook, L. J.; Shepherd, H. J.; Comyn, T. P.; Baldé, C.; Cespedes, O.; Chastanet, G.; Halcrow, M. A. Decoupled spin crossover and structural phase transition in a molecular iron (II) complex. *Chem. - Eur. J.* **2015**, *21*, 4805–4816.

(26) Money, V. A.; Carbonera, C.; Elhaïk, J.; Halcrow, M. A.; Howard, J. A.; Létard, J.-F. Interplay between kinetically slow thermal spin-crossover and metastable high-spin

state relaxation in an iron(II) complex with similar $T_{1/2}$ and T(LIESST). *Chem. - Eur. J.* **2007**, *13*, 5503–5514.

(27) Enachescu, C.; Linares, J.; Codjovi, E.; Boukheddaden, K.; Varret, F. Non-linear behaviour of the spin transition compounds during photo-excitation and relaxation. *J of Optoelectron. Adv. Mater.* **2003**, *5*, 261–266.

(28) Baldé, C.; Bauer, W.; Kaps, E.; Neville, S.; Desplanches, C.; Chastanet, G.; Weber, B.; Létard, J. F. Light-induced excited spin-state properties in 1d iron(ii) chain compounds. *Eur. J. Inorg. Chem.* **2013**, *2013*, 2744–2750.

(29) Rodríguez-Velamazán, J. A.; Carbonera, C.; Castro, M.; Palacios, E.; Kitazawa, T.; Létard, J.-F.; Burriel, R. Two-step thermal spin transition and LIESST relaxation of the polymeric spin-crossover compounds $Fe(X{-}py)_2[Ag(CN)_2]_2$ (X=H, 3-methyl, 4-methyl, 3,4-dimethyl, 3-Cl). *Chem. - Eur. J.* **2010**, *16*, 8785–8796.

(30) Chastanet, G.; Sciortino, N. F.; Neville, S. M.; Kepert, C. J. High spin to low spin relaxation regime change in a multistep 3d spin-crossover material. *Eur. J. Inorg. Chem.* **2018**, *2018*, 314–319.

(31) Shi, C.; Han, X.-B.; Zhang, W. Structural phase transition-associated dielectric transition and ferroelectricity in coordination compounds. *Coor. Chem. Rev.* **2019**, *378*, 561–576.

(32) Paez-Espejo, M.; Sy, M.; Boukheddaden, K. Elastic frustration causing two-step and multistep transitions in spin-crossover solids: Emergence of complex antiferroelastic structures. *J. Am. Chem. Soc.* **2016**, *138*, 3202–3210.

(33) Chen, Y.-C.; Meng, Y.; Dong, Y.-J.; Song, X.-W.; Huang, G.-Z.; Zhang, C.-L.; Ni, Z.-P.; Navařík, J.; Malina, O.; Zbořil, R.; Tong, M.-L. Light- and temperature-assisted spin state annealing: accessing the hidden multistability. *Chem. Sci.* **2020**, *11*, 3281–3289.

(34) Jornet-Mollá, V.; Giménez-Saiz, C.; Cañadillas-Delgado, L.; Yufit, D. S.; Howard, J. A. K.; Romero, F. M. Interplay between spin crossover and proton migration along short strong hydrogen bonds. *Chem. Sci.* **2021**, *12*, 1038–1053.

(35) Murnaghan, K. D.; Carbonera, C.; Toupet, L.; Griffin, M.; Dîrtu, M. M.; Desplanches, C.; Garcia, Y.; Collet, E.; Létard, J.-F.; Morgan, G. G. Spin-state ordering on one sub-lattice of a mononuclear iron(iii) spin crossover complex exhibiting LIESST and TIESST. *Chem. - Eur. J.* **2014**, *20*, 5613–5618.

(36) Mariette, C.; Trzop, E.; Zerdane, S.; Fertey, P.; Zhang, D.; Valverde-Munoz, F. J.; Real, J.-A.; Collet, E. Formation of local spin-state concentration waves during the relaxation from a photoinduced state in a spin-crossover polymer. *Acta. Crystallogr. B. Struct. Sci. Cryst. Eng. Mater.* **2017**, *73*, 660–668.

(37) Seredyuk, M.; Znovjyak, K.; Valverde-Muñoz, F. J.; Muñoz, M. C.; Amirkhanov, V. M.; Fritsky, I. O.; Real, J. A. Order–disorder, symmetry breaking, and crystallographic phase transition in a series of bis (trans-thiocyanate) iron(ii) spin crossover complexes based on tetradentate ligands containing 1,2,3-triazoles. *Inor. Chem.* **2023**, *62*, 9044–9053.

(38) Hôo, B.; Boukheddaden, K.; Varret, F. Two-variable macroscopic model for spin-crossover solids: Static and dynamic effects of the correlations. *Eur. Phys. J. B* **2000**, *17*, 449–457.

(39) Boukheddaden, K.; Linares, J.; Codjovi, E.; Varret, F.; Niel, V.; Real, J. Dynamical Ising-like model for the two-step spin-crossover systems. *J. Appl. Phys.* **2003**, *93*, 7103–7105.

(40) Nishino, M.; Boukheddaden, K.; Miyashita, S.; Varret, F. Arrhenius Monte Carlo study of two-step spin crossover: Equilibrium and relaxation paths. *Phy. Rev. B* **2003**, *68*, 224402.

(41) Mouri, S.; Tanaka, K.; Bonhommeau, S.; Moussa, N. O.; Molnár, G.; Bousseksou, A. Relaxation process from photoinduced states of double-step spin-crossover systems using a kinetic two-sublattice Ising-like model including intra-site coupling. *Phy. Rev. B* **2008**, *78*, 174308.

(42) Díaz-Torres, R.; Chastanet, G.; Collet, E.; Trzop, E.; Harding, P.; Harding, D. J. Bidirectional photoswitchability in an iron(iii) spin crossover complex: symmetry-breaking and solvent effects. *Chem. Sci.* **2023**, *14*, 7185–7191.

(43) Chen, Y.-C.; Meng, Y.; Dong, Y.-J.; Song, X.-W.; Huang, G.-Z.; Zhang, C.-L.; Ni, Z.-P.; Navařík, J.; Malina, O.; Zbořil, R.; Tong, M.-L. Light- and temperature-assisted spin state annealing: accessing the hidden multistability. *Chem. Sci.* **2020**, *11*, 3281–3289.

(44) Rodríguez-Velamazán, J. A.; Castro, M.; Palacios, E.; Burriel, R.; Kitazawa, T.; Kawasaki, T. A two-step spin transition with a disordered intermediate state in a new two-dimensional coordination polymer. *J. Phys. Chem. B* **2007**, *111*, 1256–1261.

(45) Ni, Z.-P.; Liu, J.-L.; Hoque, M. N.; Liu, W.; Li, J.-Y.; Chen, Y.-C.; Tong, M.-L. Recent advances in guest effects on spin-crossover behavior in Hofmann-type metal-organic frameworks. *Coord. Chem. Rev.* **2017**, *335*, 28–43.

(46) Ahmed, M. et al. Regulation of multistep spin crossover across multiple stimuli in a 2-d framework material. *Inorg. Chem.* **2022**, *61*, 6641–6649.

(47) Ahmed, M.; Arachchige, K. S. A.; Xie, Z.; Price, J. R.; Cruddas, J.; Clegg, J. K.; Powell, B. J.; Kepert, C. J.; Neville, S. M. Guest-induced multistep to single-step spin-crossover switching in a 2-d hofmann-like framework with an amide-appended ligand. *Inorg. Chem.* **2022**, *61*, 11667–11674.

(48) Nosé, S. A unified formulation of the constant temperature molecular dynamics methods. *J. Chem. Phys.* **1984**, *81*, 511–519.

(49) Nosé, S. An extension of the canonical ensemble molecular dynamics method. *Molecular Physics* **1986**, *57*, 187–191.

(50) Létard, J.-F. Photomagnetism of iron(ii) spin crossover complexes—the T(LIESST) approach. *J. Mater. Chem.* **2006**, *16*, 2550–2559.

Extended Data

Extended Data Table 1: **"Typical" values of the parameters in the model, based on previous analysis of experiments on SCO materials.**[14] Except as explicitly noted, these parameters are used in all calculations in this paper.

Parameter	**Value**
B	100 meV
C/B	4.81
Dq/B	2.039
ζ	14.6 meV
k	10.34 eV/Å^2
δ	0.1 Å
ω_{HS}	5×10^{13} s^{-1}
ω_{LS}	8×10^{13} s^{-1}
k_1	0.86 eV/Å^2
k_2	0.2 k_1
k_3	0
k_θ	0

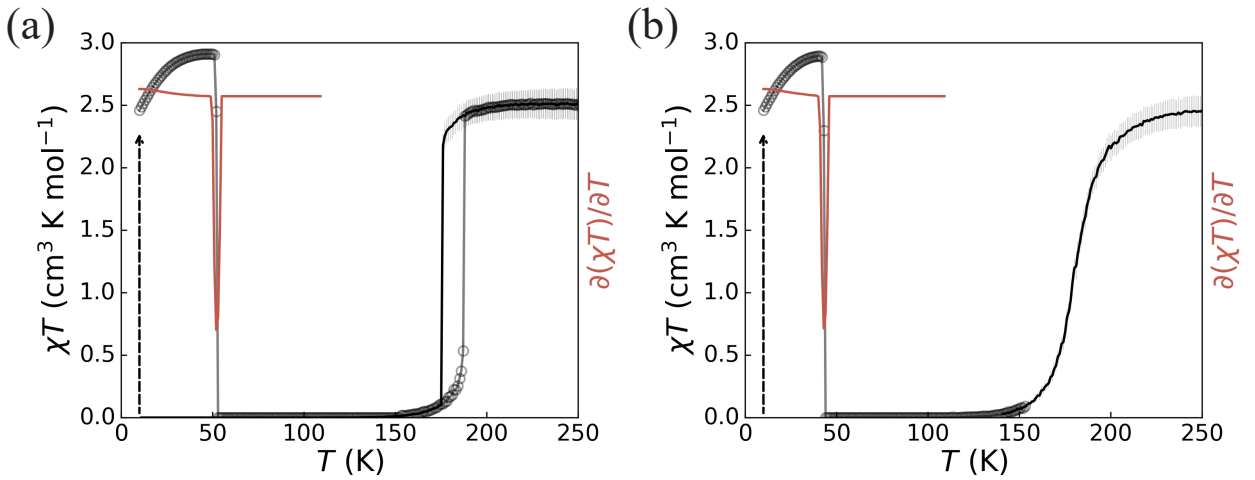

Extended Data Fig. 1: **Cooperative thermally activated decay from the trapped HS state corresponding to Fig. 2.** (a) Thermally accelerated relaxation of the trapped HS state (black circles) and the (first-order) thermal SCO transition (black lines), for the parameters given in Extended Data Table 1. $\partial(\chi T)/\partial T$ (red line) has a negative peak at $T_{\mathrm{LIESST}} = 52$ K. (b) Decreasing the intermolecualr interactions (here $k_2 = 0.06k_1$, versus $k_2 = 0.2k_1$ in (a)) drives the first order thermal SCO phase transition to a crossover and decreases T_{LIESST} to 43 K.

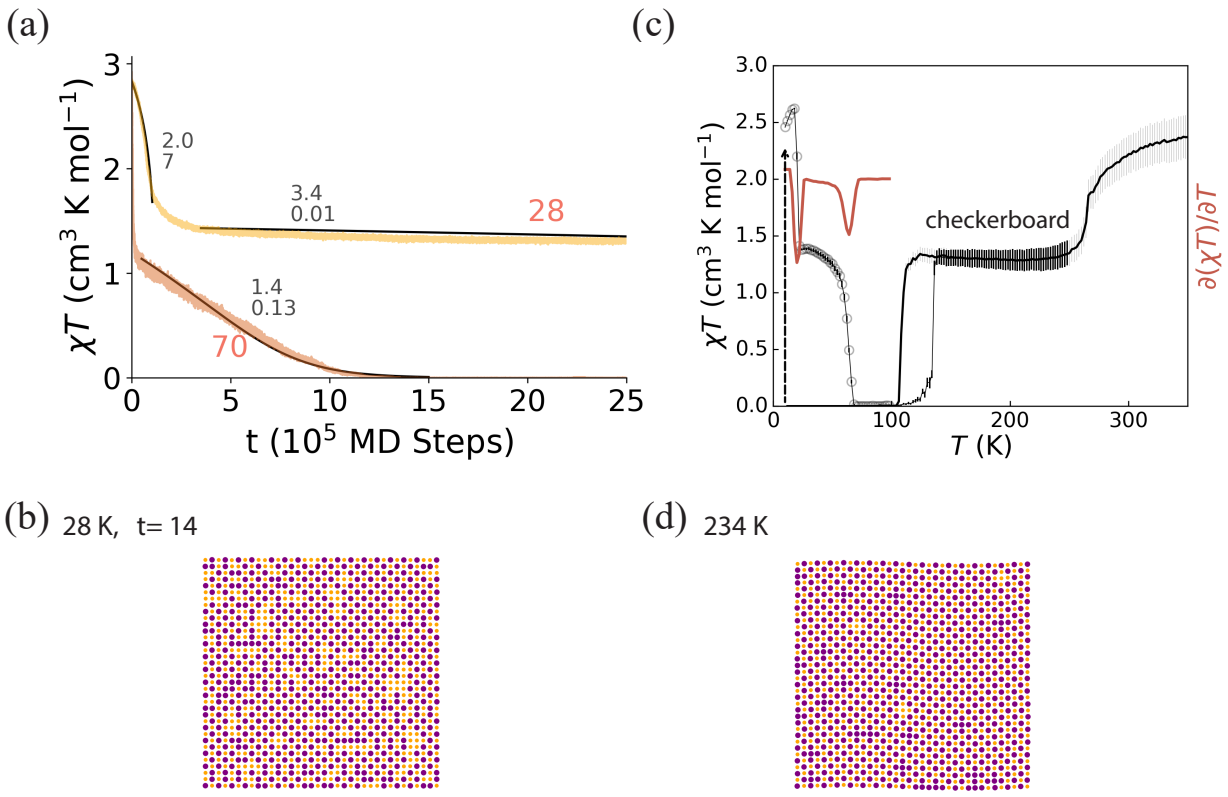

Extended Data Fig. 2: **Two-step relaxation involving checkerboard intermediate spin-state order is similar to two-step relaxation with stripe intermediate order (Fig. 3).** (a) Isothermal relaxation is sigmoidal for both steps (black lines). (b) A typical snapshot of the short-range checkerboard state that appears at the intermediate plateau during isothermal reactions. (c) The two-step thermal transition with a long-range ordered, symmetry-breaking, checkerboard phase in the intermediate plateau. Similarly, the thermally accelerated relaxation of the trapped HS state is two step. Thus, $\partial(\chi T)/\partial T$ has two negative peaks. (d) A typical spin-state configuration at the intermediate step during the cooling sweep of thermal SCO. Here $k_2 = 0.15k_1$, $k_3 = -0.20k_1$ and $Dq/B = 2.0503$.

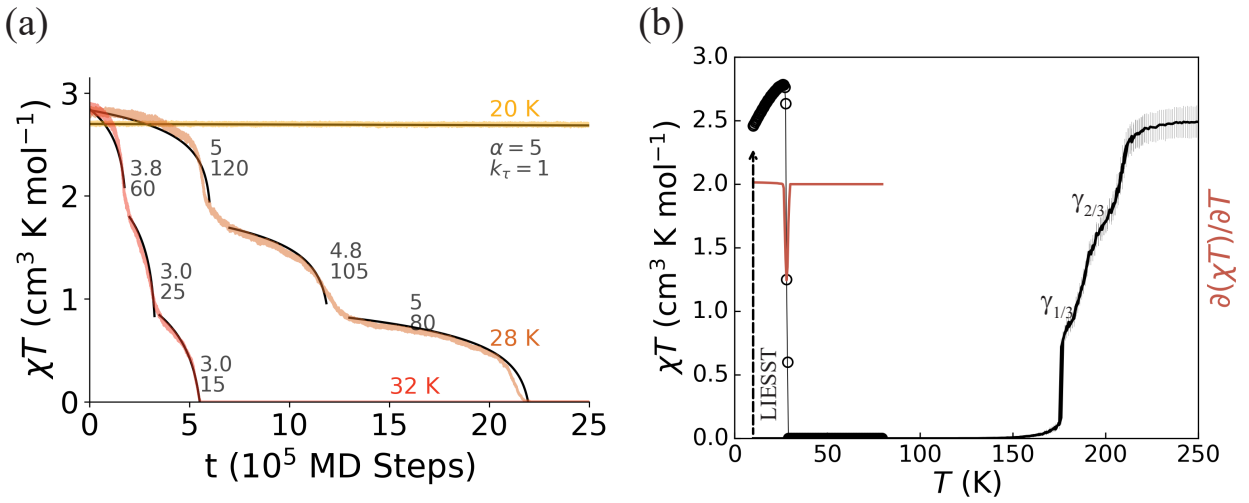

Extended Data Fig. 3: **Complete, three-step relaxation involving two intermediate plateaus.** Multiple steps are also found in the isothermal relaxation. Here $Dq/B = 2.0459$ $k_1 = 1.55\text{eV}/\text{Å}^2$, $k_2 = -0.21k_1$, $k_3 = 0.1k_1$, and $k_\theta = 0.56k_1$.